Monitoring LSO/LYSO Crystal Calorimeters

Fan Yang, *Member, IEEE*, Liyuan Zhang, *Member, IEEE*, and Ren-Yuan Zhu, *Senior Member, IEEE*

***Abstract*—LSO/LYSO crystals were chosen by the SuperB, Mu2e and COMET experiments to construct total absorption electromagnetic calorimeters. They were also proposed as the active medium for a Shashlik calorimeter which was one of the two options proposed for the CMS forward calorimeter upgrade at the proposed HL-LHC. Because of the severe radiation environment expected at the HL-LHC, precision light monitoring is crucial for keeping excellent energy resolution promised by LYSO crystals. This paper discusses the wavelength choice for monitoring LYSO based crystal calorimeters. γ-ray induced absorption and light output loss were measured for 20 cm long crystals from five different vendors. Monitoring sensitivity and divergence are analyzed. Two approaches using excitation and emission light and their practical implementations in a beam test at Fermilab are discussed. The response of an LYSO/W Shashlik calorimeter cell after a γ-ray irradiation of 90 Mrad is also presented.**

***Index Terms*—Calorimeter, crystal, monitoring, radiation damage.**

I. Introduction

BECAUSE of their high stopping power, fast and bright scintillation and superb radiation hardness against γ-rays, neutrons and charged hadrons cerium doped lutetium oxyorthosilicate (Lu_2SiO_5:Ce or LSO) [1] and cerium doped lutetium yttrium oxyorthosilicate ($Lu_{2(1-x)}Y_{2x}SiO_5$:Ce or LYSO) [2], [3] crystals were chosen by the SuperB, Mu2e and COMET experiments to construct total absorption electromagnetic calorimeters. They were also proposed as the active medium for a Shashlik calorimeter which was one of the two options proposed for the CMS forward calorimeter upgrade at the HL-LHC [4], [5]. Precision light monitoring is crucial for keeping excellent energy resolution promised by the LYSO crystals in severe radiation environment, such as the HL-LHC. It can be carried out by injecting light pulses with a wavelength around crystal's emission peak, such as the CMS PWO ECAL [7], or around photo-excitation peak, such as the PHENIX Lead-Scintillator sampling ECAL [8]. This paper discusses the wavelength choice for monitoring LYSO based crystal calorimeters. γ-ray induced absorption and light output loss were measured for 20 cm long crystals from five different vendors. Monitoring sensitivity and divergence are analyzed. The pros and cons of the two monitoring approaches using excitation and emission light and their practical implementations in a beam test at Fermilab are discussed. The response of an LYSO/W Shashlik calorimeter cell after a γ-ray irradiation of 90 Mrad is also presented.

Fig. 1. A photo showing five LYSO crystals of $2.5 \times 20 \times 2.5$ cm^3.

II. Monitoring Wavelength Choice

Fig. 1 is a photo showing five samples used in the investigation of monitoring wavelength. They all have the same dimensions of $2.5 \times 20 \times 2.5$ cm^3 and are from 5 different vendors from top to bottom: Crystal Photonics, Inc. (CPI), CTI Molecular Imaging (CTI), Saint-Gobain Ceramics & Plastics, Inc. (SG), Shanghai Institute of Ceramics (SIC) and Sichuan Institute of Piezoelectric and Acousto-optic Technology (SIPAT) respectively. Light output (LO), light response uniformity (LRU) and longitudinal transmittance (LT) were measured at room temperature before and after γ-ray irradiations in five steps between 10^2 and 10^6 rad. LO was measured by using a Hamamatsu R1306 PMT with a coincidence trigger from a ^{22}Na source with systematic uncertainty in repeated measurements of about 1% [9]. LT spectra were measured by a Perkin Elmer Lambda-950 UV/Vis/NIR spectrophotometer with double beam, double monochromator and an integrating sphere in a large sample compartment. The systematic uncertainty in repeated measurements is about 0.15%. γ-ray irradiations were carried out at two irradiation facilities at Caltech: an open ^{60}Co source and a closed ^{137}Cs source. The former provides dose rates between 2 and 100 rad/h by placing samples at appropriate distances. The later provides a dose rate of 8,500 rad/h with 5%

Manuscript received July 20, 2015; revised November 16, 2015; accepted December 15, 2015. Date of publication March 30, 2016; date of current version April 15, 2016. This work was supported in part by the U.S. Department of Energy Grant DE-SC0011925.

The authors are with the California Institute of Technology, Pasadena, CA 91125 USA (e-mail: zhu@hep.caltech.edu).

Color versions of one or more of the figures in this paper are available online at http://ieeexplore.ieee.org.

Digital Object Identifier 10.1109/TNS.2015.2510581

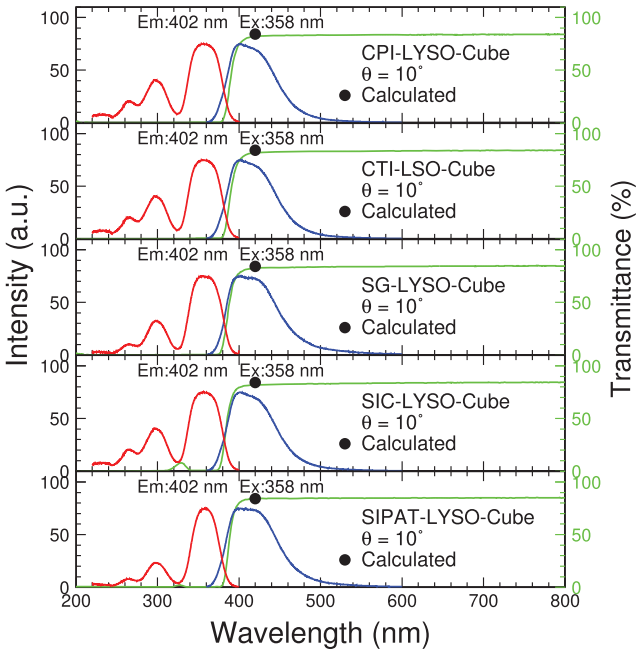

Fig. 2. Excitation, photo luminescence (left scale) and transmittance spectra (right scale) are shown as a function of wavelength for five LSO/ LYSO cubes of 17 cm from different vendors.

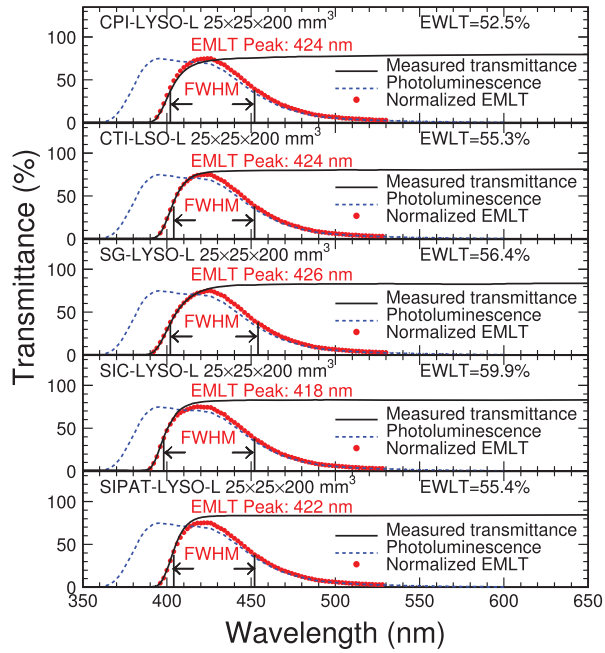

Fig. 3. Photo luminescence, longitudinal transmittance and normalized emission multiplied longitudinal transmittance spectra are shown for five LSO/LYSO samples from different vendors.

uniformity along sample's longitudinal axis when samples are placed at the center of the irradiation chamber [10].

Fig. 2 shows excitation, photo-luminescence (PL) and LT spectra for the five LSO/LYSO cubes of 1.7 cm from different vendors. The spectra are consistent with an excitation peak at 358 nm and an emission peak at 402 nm. The PL photo-luminescence spectra were measured by using a HITACHI F4500 fluorescence spectrophotometer. The angle between the excitation UV light and the sample was set to be 10° so that the photo-luminescence spectra collected are not affected by internal bulk absorption [11]. The cut-off wavelength of the transmittance is red-shifted for long samples because of the self-absorption. Also shown in the figure is the theoretical transmittance at 420 nm calculated by using the refractive index. The difference between the measured LT and the theoretical value indicates the degree of absorption and/or scattering. Emission multiplied longitudinal transmittance (EMLT) is shown in Fig. 3, which represents the intensity of scintillation light in the crystal. The average of the EMLT peak wavelength is 423 nm with a FWHM of 48 nm. Also listed in the figure is emission weighted longitudinal transmittance (EWLT) [10], which represents crystal's transparency for the entire emission spectrum.

Fig. 4 shows the LT spectra in an expanded scale and the EWLT values measured before and after γ-ray irradiations of 10^2, 10^4 and 10^6 rad for five LYSO samples. The transmittance loss is small and mostly at short wavelengths. The initial LO and LRU before γ-ray irradiation are shown in Fig. 5 for five samples. All samples have good LO with LRU of better than 3%, indicating that the self-absorption effect is more or less compensated by optimizing Ce doping [5]. Fig. 6 shows LO and LRU of CPI-LYSO after γ-ray irradiations of 10^2, 10^4 and 10^6 rad. With LRU more or less maintained, its LO shows a loss of about 11% after 10^6 rad. Similar to CPI-LYSO, other four samples

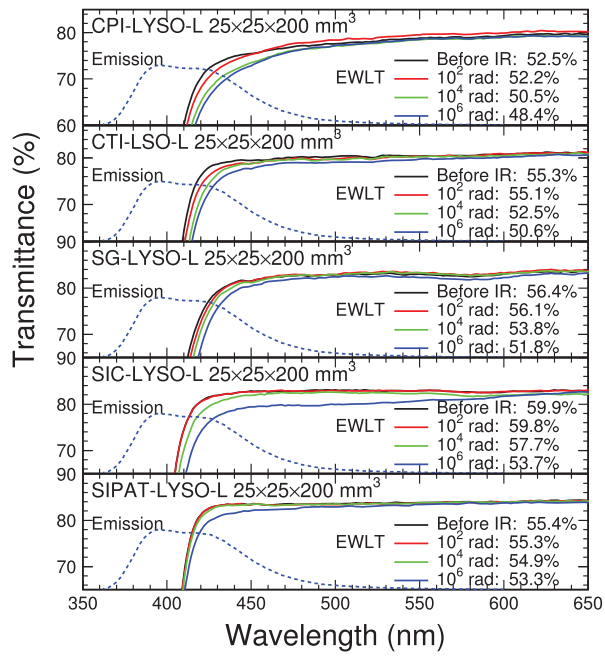

Fig. 4. The transmittance and photo-luminescence spectra are shown as a function of wavelength for the five LSO/LYSO samples before and after irradiations with integrated doses of 10^2, 10^4 and 10^6 rad.

also show unchanged LRU after 10^6 rad. The losses of EWLT and LO observed in five samples after 1 Mrad are summarized in Table I. An average of 7.7% and 12.9% was observed for EWLT and LO respectively, indicating excellent radiation hardness of LSO/LYSO crystals.

Assuming scintillation mechanism is not damaged, light pulses with a wavelength close to the emission peak would be effective to monitor variations of crystal transparency. CMS at LHC, for example, chooses 440 nm for PWO crystal monitoring

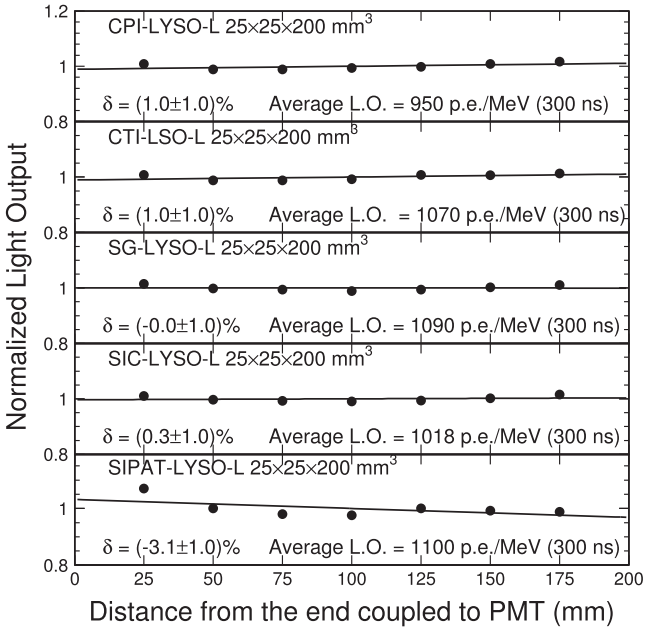

Fig. 5. Initial light output and longitudinal response uniformity measured for 5 LYSO samples.

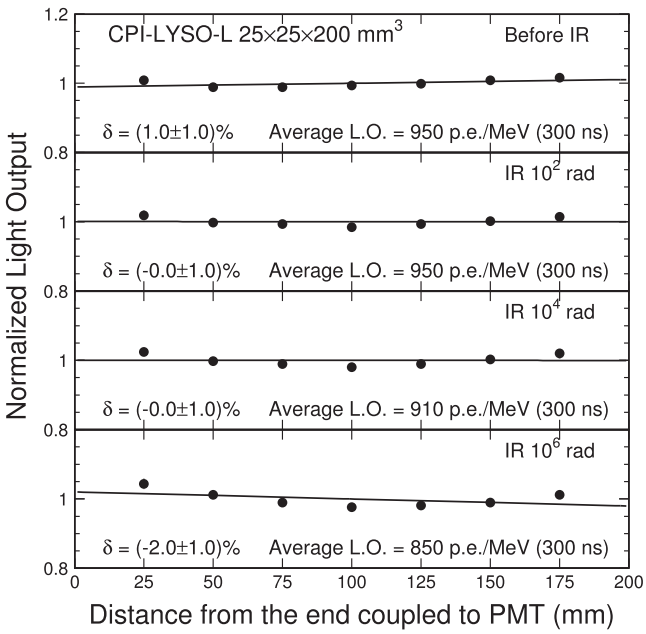

Fig. 6. Light output and light response uniformities measured before and after irradiation with integrated doses of 10^2, 10^4 and 10^6 rad are shown for CPI-LYSO.

TABLE I
EWLT AND LO LOSSES AFTER 1 MRAD OF FIVE LSO/LYSO SAMPLES

Sample	EWLT loss (%)	LO loss (%)
CPI-LYSO-L	7.8	10.5
CTI-LSO-L	8.5	12.1
SG-LYSO-L	8.2	15.6
SIC-LYSO-L	10.4	14.3
SIPAT-LYSO-L	3.8	11.8
Average	7.7	12.9

[7]. In this case, monitoring sensitivity, defined as the ratio between the normalized LT loss and the normalized LO loss,

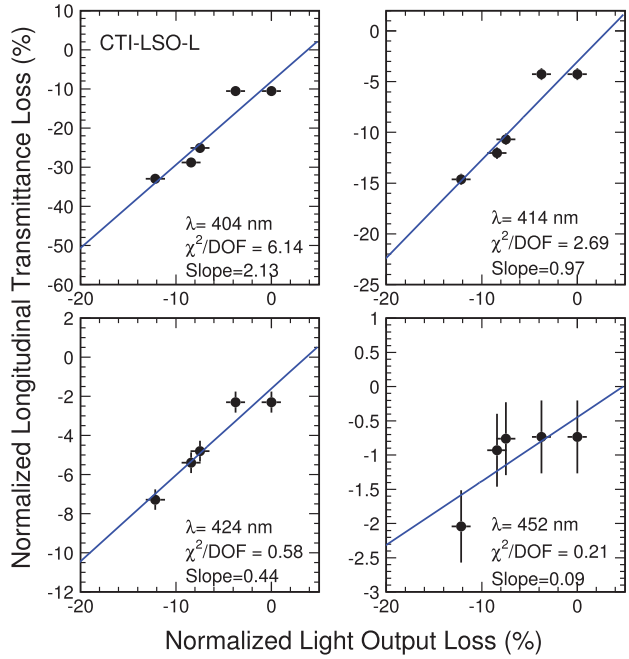

Fig. 7. LT loss versus LO loss of CTI-LSO at 4 wavelengths and fits.

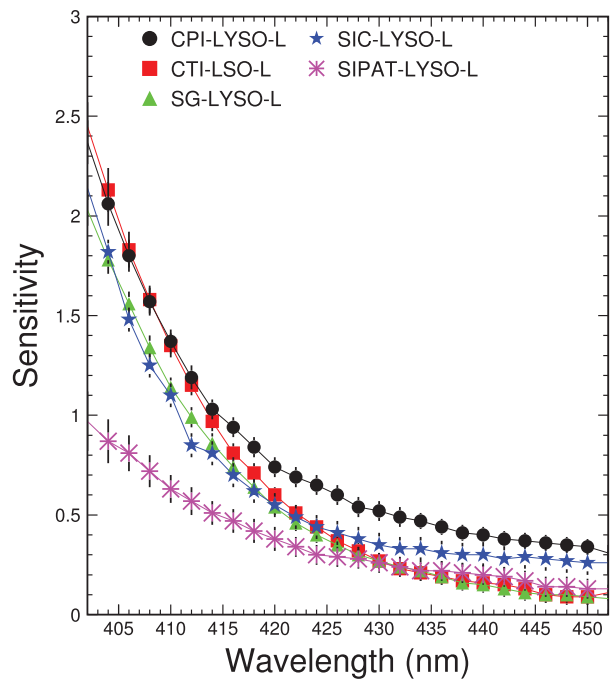

Fig. 8. Monitoring sensitivities are shown as a function of wavelength for five LSO/LYSO samples.

is a function of monitoring wavelength. Similar to what was done for the CMS PWO crystals, linear fits were carried out at each wavelength for each crystal sample. Fig. 7 shows the fits for the CTI-LSO sample at 404, 414, 424 and 452 nm. The fitted slope represents the monitoring sensitivity. Fig. 8 shows the monitoring sensitivities as a function of wavelength for five samples. It's clear that the monitoring sensitivity increases at shorter wavelengths, the monitoring signal intensity represented by EMLT shown in Fig. 3, however, indicates that the efficiency of light propagation is low at shorter wavelengths.

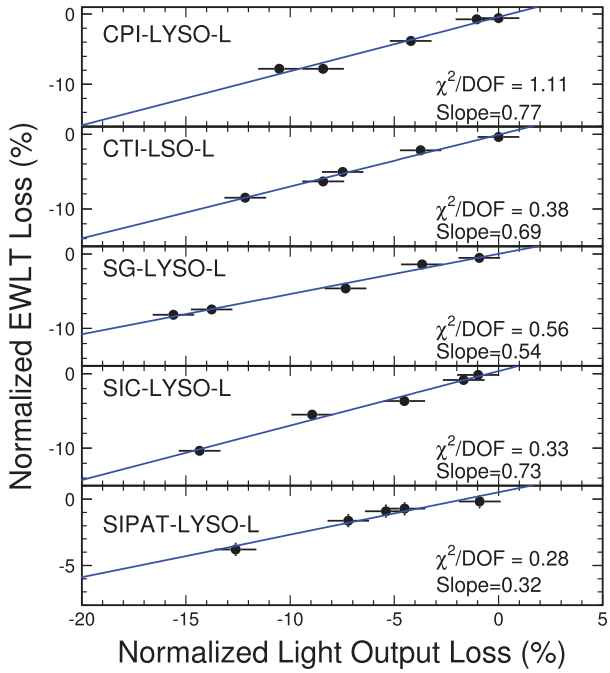

Fig. 9. EWLT loss versus LO loss and corresponding linear fits are shown for the five LSO/LYSO samples.

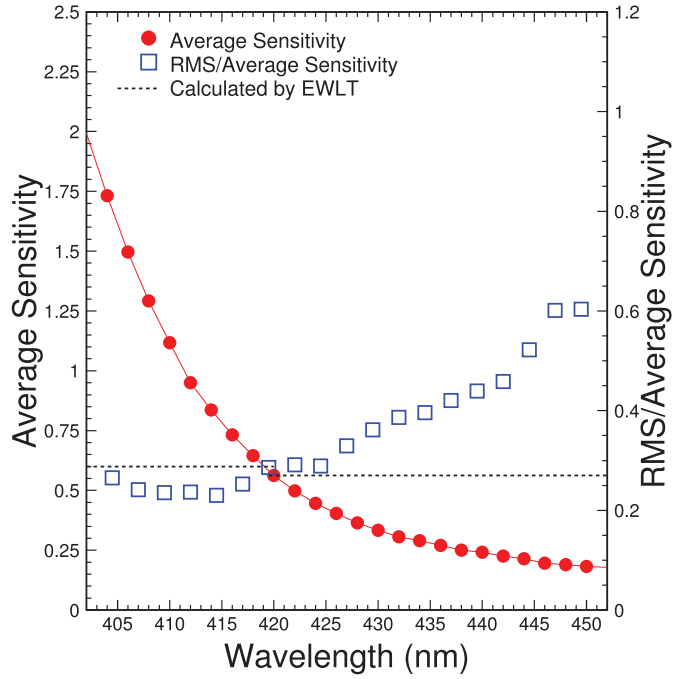

Fig. 10. Average sensitivity and its divergence as a function of wavelength as well as the result using EWLT.

Another monitoring approach uses light pulses with a wavelength around excitation peak, so that the monitoring light covers the entire emission spectrum. The PHENIX experiment at RHIC, for example, chooses 355 nm from a Nd:YAG laser to monitor variations of plastic scintillators [8]. This approach monitors both crystal transparency and photo-luminescence production. Its monitoring sensitivity may be evaluated by fitting the EWLT loss versus the LO loss as shown in Fig. 9.

Fig. 10 compares monitoring sensitivity for two monitoring approaches. The solid dots (left scale) in the plot represent monitoring sensitivity as a function of wavelength for the emission approach. The open squares (right scale) in the plot represent the divergence between 5 samples, which is defined as the rms of the sensitivities. The dashed lines show sensitivity and divergence for the excitation approach. It is clear that the monitoring sensitivity is consistent between two approaches at 423 nm or the peak of EMLT. Consequently, 423 nm is chosen as the monitoring wavelength for the emission approach. On the other hand, 355 nm may be chosen for the excitation approach as shown in Fig. 2. A consistent divergence at 25% level is observed for both approaches for five crystals from different vendors.

III. Monitoring LYSO/W Shashlik Calorimeter

Fig. 11 shows an LYSO/W Shashlik cell with thirty LYSO plates of $14 \times 14 \times 1.5$ mm^3 and twenty nine tungsten plates of $14 \times 14 \times 2.5$ mm^3 interleaved with 15 μm thick Al foils. The Al foils is chosen as the reflective layer for LYSO plates because of its excellent radiation hardness. The scintillation light in LYSO plates was wavelength shifted and transported in four Y-11 WLS fibers of 1 mm diameter. To allow the Y-11 WLS fiber through, four holes of 1.3 mm diameter were drilled through the LYSO and W plates at four positions with distances of 3.5 mm to the edges of the plate. A hole of 0.9 mm

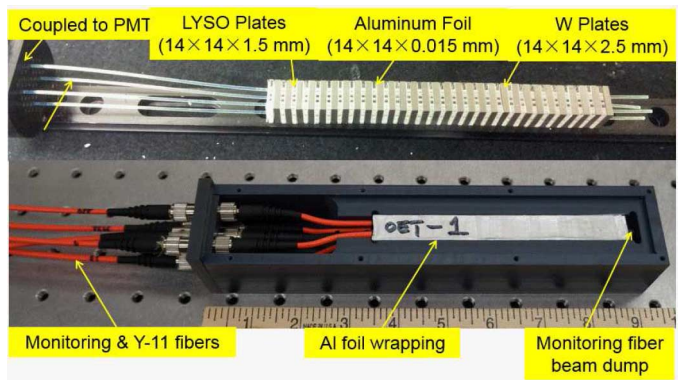

Fig. 11. A photo showing a Shashlik cell during (top) and after (bottom) assembly.

in diameter was drilled at the center of the plate to introduce monitoring light pulses via a leaky quartz fiber [5].

Two LYSO/W Shashlik cells were constructed: the SIC-C1 cell uses LYSO plates from SICCAS and the OET-C1 cell uses LFS plates from Beijing Opto-Electronics Technology Co. Ltd. (BOET). Both cells were irradiated by Co-60 γ-ray at JPL to 90 Mrad with radiation damage monitored by using a 420 nm LED based light monitoring system as shown in Fig. 12. The monitoring light from a blue LED (Thorlabs M420F) was collimated, chopped and splitted by a beam sampler, and then injected into the Shashlik cell through a 365 μm optical fiber inserted in the central hole of the cell. While the final design of the leaky quartz fiber is still under development, quartz fibers with jacket removed were used in this investigation. Natural scattering light from the fiber delivered photons into LYSO layers with the fiber end coupled to a beam dump. The four Y-11 WLS fibers were read out by a PMT (Hamamatsu R2059). The splitted beam was read out by a PIN photodiode (Thorlabs DET10A)

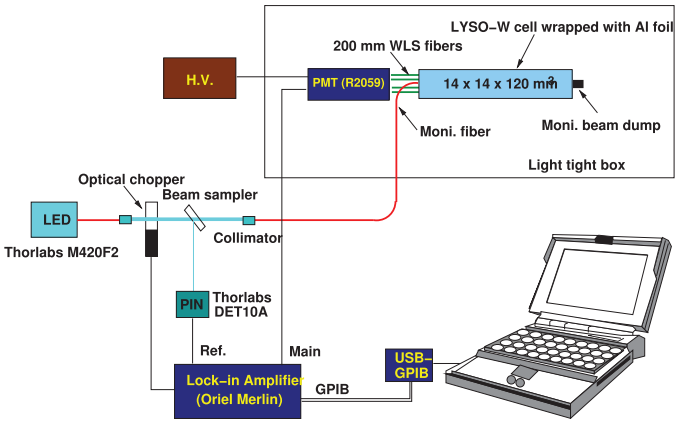

Fig. 12. A schematic showing the set-up used for measuring the LYSO-W-Al Shashlik cell before and after γ-ray irradiation.

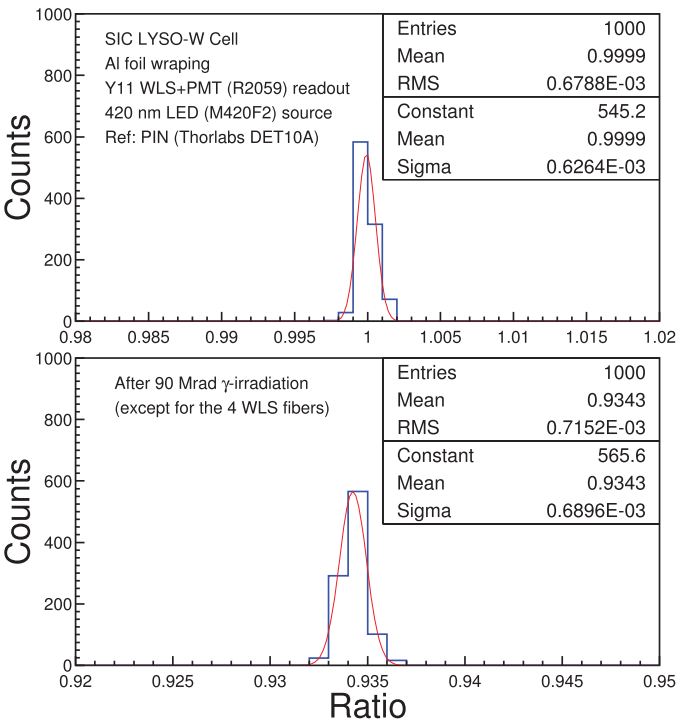

Fig. 13. The measured monitoring signals of the LYSO-W-Al Shashlik made by SIC LYSO plates before and after 90 Mrad γ-ray irradiation.

serving as a reference. A lock-in amplifier (Oriel Merlin) measured the ratio of the PMT signal over the PIN signal with noise suppressed to a level of 10^{-3}. The systematic uncertainties for repeated measurements are about 1% and 3% respectively without and with replacing four Y-11 WLS fibers.

Fig. 13 shows the monitoring response of the SIC-C1 Shashlik cell before and after 90 Mrad irradiation at 1 Mrad/h with four Y-11 WLS fibers replaced. The results of the two cells after 90 Mrad irradiation are summarized in Table II. Consistent degradations at a level of 70% are observed in two LYSO/W Shashlik cells with irradiated Y-11 fibers, which are reduced to 6.5% after Y-11 fibers replaced. While the liquid scintillator based quartz capillary WLS is still under development, preliminary irradiation results show a damage level of much less than Y-11 fibers [6]. A light monitoring system is crucial

TABLE II
MONITORING SIGNALS OF TWO LYSO/W SHASHLIK CELLS AFTER 90 MRAD IRRADIATION

LYSO-W-Al Shashlik Cell	Y-11 WLS Fibers	LED Response (%)
SIC-C1	Irradiated	29 ± 1
SIC-C1	Replaced	93 ± 3
OET-C1	Irradiated	30 ± 1
OET-C1	Replaced	94 ± 3

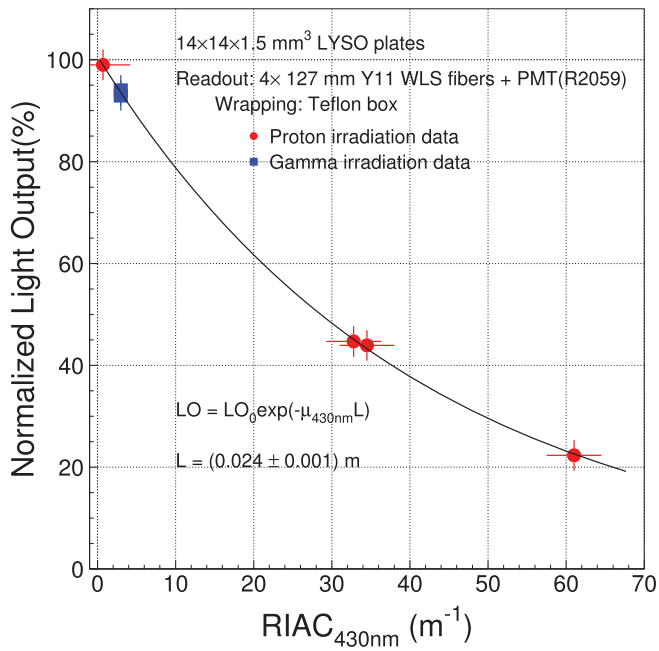

Fig. 14. Light output versus radiation induced absorption at 430 nm and exponential fit in $14 \times 14 \times 1.5$ mm^3 LYSO plates.

to correct response of the LYSO/W/Quartz Capillary Shashlik cells, including degradations of LYSO plates, quartz capillaries and photo-detectors, *insitu* at the proposed HL-LHC.

The transmittance and light output of the LYSO and LFS plates in these two Shashlik cells were measured after the irradiation. The average light output loss and radiation induced absorption coefficients were found to be consistent with that of proton irradiated plates. Fig. 14 shows the normalized light output as a function of the measured radiation induced absorption coefficient for $14 \times 14 \times 1.5$ mm^3 LYSO/LFS plates, which can be fitted by a simple exponential component with an optical path length of about 2.4 cm, indicating that the radiation damage in these plates is caused by radiation induced absorption so can be corrected by light monitoring.

IV. LASER BASED MONITORING SYSTEM FOR LYSO/W SHASHLIK BEAM TEST

A laser based light monitoring system was built at Caltech and tested for a 4×4 LYSO/W Shashlik matrix beam test at Fermilab.

Fig. 15 shows a schematic for an OPOTEK Opolette 355 II laser based monitoring system. The OPOTEK laser uses optical parametric oscillator (OPO) technology, and provides laser pulses at 20 Hz with intensity of 3.5 and 2.5 mJ respectively at 355 and 425 nm. The laser pulses were coupled to a 30 m long quartz fiber, and then distributed into 18 optical fibers via

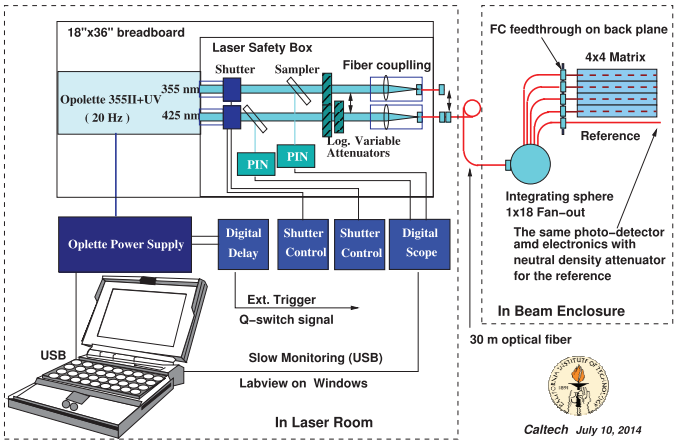

Fig. 15. A schematic showing an OPOTEK OPO laser system used for the Shashlik test beam at Fermilab.

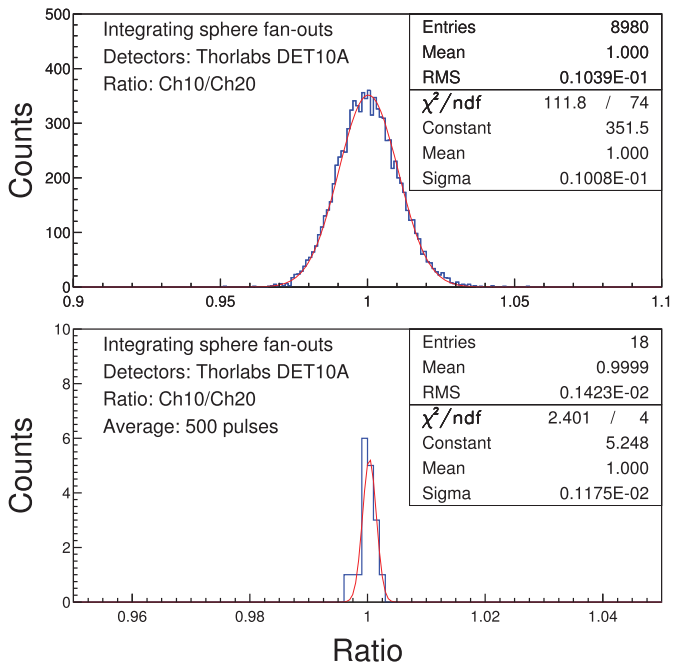

Fig. 16. Measured monitoring precision, or ratio between two channels readout by using the same photo-detectors, is shown in pulse to pulse (top) and with an average of 500 pulses (bottom).

a home-made Teflon based integrating sphere. 16 fibers were used to inject laser pulses into the 16 channels of the 4×4 LYSO/W test beam matrix. The other 2 fibers were used as reference. The reference channels were attenuated by neutral density filters and then read out by the same photo-detector and electronics as that of the Shashlik matrix to minimize systematic effect to the monitoring precision. With no radiation damage at Fermilab this system was used for debugging and mapping readout channels, studying amplifier pulse shapes, and calibration with single photo-electrons.

Fig. 16 shows monitoring precision, measured as the ratio between two channels readout with PIN photodiodes (Thorlabs DET10A). While the pulse to pulse monitoring precision is about 1% (top), 0.1% was achieved with average of 500 pulses (bottom).

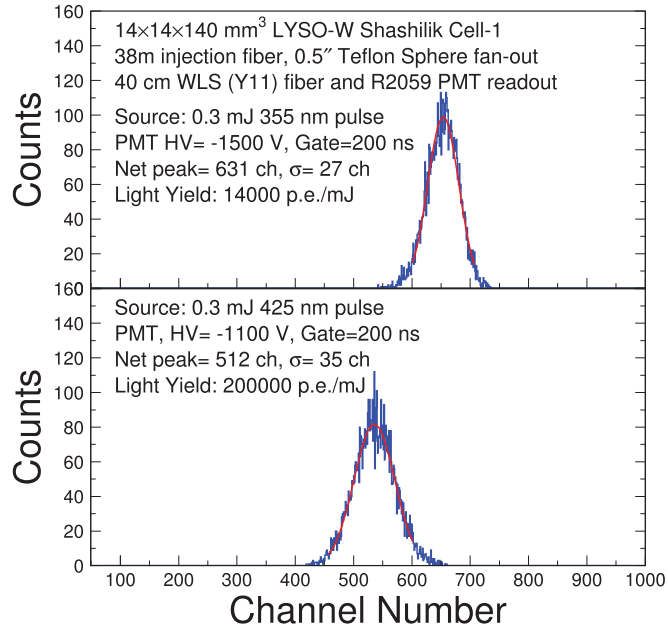

Fig. 17. The measured monitoring dynamic range at 355 (top) and 425 (bottom) nm of the OPO laser system used in the Shashlik test beam at Fermilab.

Fig. 17 shows the monitoring dynamic range at 355 (top) and 425 (bottom) nm respectively measured by the monitoring setup. A factor of 15 lower dynamic range for 355 nm was observed, which is caused by the conversion from excitation to emission. Since there is no commercial laser available around 425 nm, a pulsed laser at 425 nm would have to be custom made. On the other hand, commercial DPSS lasers at 355 nm with a pulse energy of 15 times of that at 425 nm are available by using the frequency triple technology. Attention, however, should be paid to possible damage in optical system for using lasers at 355 nm.

High light yield of LYSO crystals requires high light pulse intensity to reach high dynamic range for a LYSO-W Shashlik calorimeter. It thus is important to reduce the total loss is the entire optical chain from the laser to each individual calorimeter cells. Table III summarizes light losses between laser to calorimeter cell in two existing monitoring systems for the CMS and PHENIX ECALs.

After removing the excitation to emission conversion efficiency (UV-VIS in Table III) the PHENIX system has a total attenuation of 74.5 dB, which is consistent with the 72 dB of the CMS ECAL monitoring system. Fig. 18 shows a preliminary design for an LYSO/W Shashlik calorimeter. This design modifies the existing CMS ECAL light monitoring system by replacing the level-2 fan-outs with an optical switch. Since typical insertion loss of an optical switch is about 2 dB, the total loss of the optical chain would be reduced by 15 dB. Since radiation damage in LYSO crystals does not recover and is much smaller than that in PWO crystals it is feasible to reduce the monitoring frequency for LYSO crystals from the half hour required for the CMS PWO ECAL [7]. The design in Fig. 18 provides a dynamic range of 140 GeV for an LYSO crystal based total absorption calorimeter for laser pulses of 1 mJ at 425 nm. For the proposed LYSO/W Shashlik

TABLE III
LIGHT LOSSES IN THE MONITORING SYSTEMS OF THE CMS [7] AND PHENIX [8] ECALS

CMS PWO ECAL Monitoring at 440/447 nm (dB)				PHENIX ECAL (Lead Scintillator) Monitoring at 355 nm (dB)			
	Fanout	Extra	Total		Fanout	Extra	Total
LSDS	0	13	13	LSDS	7.8	0.1	7.9
Optical fiber (150 m)	0	3.0	3.0	Optical fiber (50 m)	0	3.0	3.0
Level 2 (1:7)	8.5	8.5	17	Level 1 (1:21)	13.3	12.2	25.5
Level 1 (1:240)	24	15	39	Level 2 (1:38)	15.8	10.8	26.6
				Module eff. (UV-VIS)	0	31.2	31.2
				Connections	0	11.5	11.5
Total	32.5	39.5	72		36.9	68.8	105.7

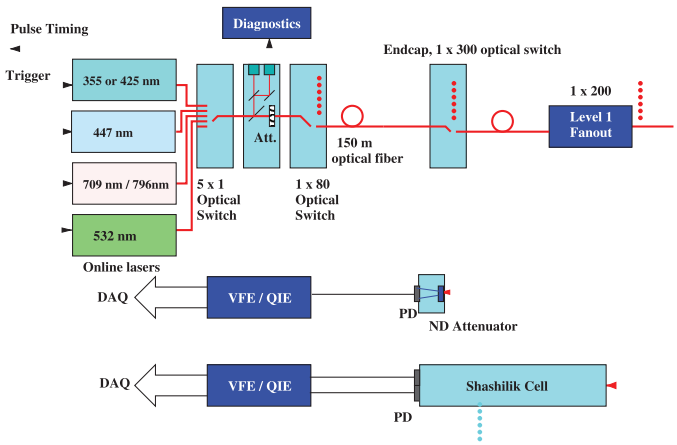

Fig. 18. A schematic showing a conceptual design of the Shashlik calorimeter monitoring for CMS.

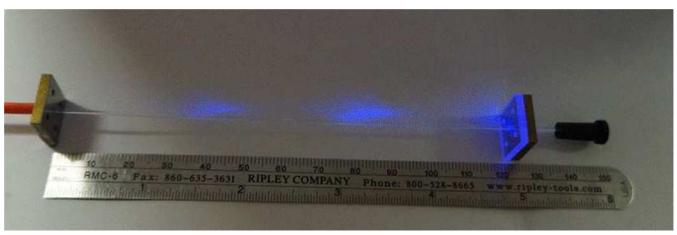

Fig. 19. A photo showing a preliminary result of a mechanically scribed quartz fiber.

calorimeter, sampling fraction and leaky fiber efficiency should also be taken into account. With a typical sampling fraction of 0.2, or a factor of 5, and a 15% efficiency of the leaky fiber (or loss < 8 dB), a dynamic range of 110 GeV can be achieved.

R&D for a high efficient and radiation hard light injection system is under the way. Because of its excellent radiation hardness leaky quartz fiber or quartz rod is under investigation for LYSO/W Shashlik calorimeter monitoring. Fig. 19 shows a preliminary result obtained by mechanically scribed quartz fiber. Chemical or laser etching as well as optimization of the level-1 fan-out unit will also be investigated.

V. SUMMARY

LSO/LYSO crystals suffer from transparency loss under γ-ray and proton irradiation which leads to light output loss. A light monitoring system is crucial for keeping precision of the proposed LYSO crystal based calorimeters. The monitoring wavelengths for LYSO are 425 nm and 355 nm respectively for monitoring transparency only and both excitation and transparency. Because of no recovery and small damage level, the required monitoring frequency for the proposed LYSO/W Shashlik calorimeter is much lower than the 0.5 hour required for the CMS PWO ECAL. By replacing the level 2 fanouts with an optical switch, a dynamic range of 100 GeV can be achieved by using commercial lasers with 1 or 15 mJ/pulse respectively for the emission or excitation approaches. Additional work is required to develop an effective light leaking system and level 1 splitter.

REFERENCES

[1] C. Melcher and J. Schweitzer, "Cerium-doped lutetium oxyorthosilicate: A fast, efficient new scintillator," *IEEE Trans. Nucl. Sci.*, vol. 39, no. 4, pp. 502–505, Aug. 1992.

[2] D. Cooke, K. McClellan, B. Bennett, J. Roper, M. Whittaker, and R. Muenchausen, "Crystal growth and optical characterization of cerium-doped $Lu_{1.8}Y_{0.2}SiO_5$," *J. Appl. Phys.*, vol. 88, pp. 7360–7362, 2000.

[3] T. Kimble, M. Chou, and B. Chai, "Scintillation properties of LYSO crystals," *Proc. IEEE Nuclear Science Symp. Conf.*, vol. 3, pp. 1434–1437, 2002.

[4] R.-Y. Zhu, "The next generation of crystal detectors," in *Proc. 16th Int. Conf. Calorimetry in High Energy Physics*, 2014, p. 012055, 10.1088/1742-6596/587/1/012055, J. Physics, Conf. Ser. 587.

[5] L. Zhang, R. Mao, F. Yang, and R.-Y. Zhu, "LSO/LYSO crystals for calorimeters in future HEP experiments," *IEEE Trans. Nucl. Sci.*, vol. 61, no. 1, pp. 483–488, Feb. 2004.

[6] B. W. Baumbaugh, K. Ford, M. McKenna, D. Ruggiero, R. Ruchti, and M. Vigneault1, "Studies of wavelength-shifting liquid filled quartz capillaries for use in a proposed CMS calorimeter," presented at the IEEE NSS/MIC Conf., San Diego, CA, USA, Nov. 4, 2015, Paper N3D1-2.

[7] M. Anfreville *et al.*, "Laser monitoring system for the CMS lead tungstate crystal calorimeter," *Nucl. Instrum. Methods Phys. Res. A*, vol. 594, pp. 292–320, 2008.

[8] G. David *et al.*, "The calibration and monitoring system for the PHENIX lead-scintillator electromagnetic calorimeter," *IEEE Trans. Nucl. Sci.*, vol. 45, no. 3, pp. 705–709, Jun. 1998.

[9] J. Chen, R. Mao, L. Zhang, and R. Y. Zhu, "Large size LSO and LYSO crystals for future high energy physics experiments," *IEEE Trans. Nucl. Sci.*, vol. 54, no. 3, pp. 718–724, Jun. 2007.

[10] J. Chen, R. Mao, L. Zhang, and R. Y. Zhu, "Gamma-ray induced radiation damage in large size LSO and LYSO crystal samples," *IEEE Trans. Nucl. Sci.*, vol. 54, no. 4, pp. 1319–1326, Jun. 2007.

[11] R. Mao, L. Zhang, and R. Y. Zhu, "Emission spectra of LSO and LYSO crystals excited by UV light, X-Ray and γ–ray," *IEEE Trans. Nucl. Sci.*, vol. 55, no. 3, pp. 1759–1766, Jun. 2008.

[12] X. Qu, L. Zhang, and R. Y. Zhu, "Radiation induced color centers and light monitoring for lead tungstate crystals," *IEEE Trans. Nucl. Sci.*, vol. 47, no. 6, pp. 1741–1747, Dec. 2000.